LA-UR-19-24978
Approved for public release; distribution is unlimited.

Title: Models Predicting Void Swelling Incubation Dose as a function of Irradiation Conditions

Author(s): Kohnert, Aaron Anthony
van Couvering, G.
Was, G. S.
Wirth, Brian D.

Intended for: Report

Issued: 2019-05-30

Models Predicting Void Swelling Incubation Dose as a function of Irradiation Conditions

Fuel Cycle Research & Development

Prepared for
U.S. Department of Energy
Advanced Fuels Campaign

A.A. Kohnert, LANL
G. van Couvering, U. Michigan
G.S. Was, U. Michigan
B.D. Wirth, UT- Knoxville

11/30/2018

L3 Milestone Report: M3NT-18LA110102194
Models Predicting Void Swelling Incubation Dose as a function of Irradiation Conditions

A.A. Kohnert[1,2], G. van Couvering[3], G.S. Was[3], and B.D. Wirth[1]
[1] University of Tennessee, Knoxville
[2] Los Alamos National Laboratory
[3] University of Michigan

30 November 2018

Executive Summary

This report documents the development status of a cluster dynamics model to predict microstructural evolution in high-energy particle irradiated ferritic martensitic steels, in which we have recently implemented a model for the biased absorption of self-interstitial defects at small, nanometer-sized cavities that can provide an intrinsic nucleation barrier for the onset of void swelling. Following a brief review of the cluster dynamics modeling approach, this report describes the atomistic modeling results that demonstrate this phenomena, along with an investigation on the influence of helium content on modifying the intrinsic cavity bias. Subsequently, the report describes the initial results obtained from our cluster dynamics modeling of the incorporation of this cavity bias on the predicted swelling incubation dose as a function of irradiation temperature. Finally, the report concludes with a discussion of the remaining modeling research required to fully validate the model for application to high dose neutron or ion beam irradiation exposure conditions.

I. Introduction

Exposure of metallic structural materials to irradiation environments results in significant microstructural evolution, property changes and performance degradation, which limits the extended operation of current generation light water reactors and restricts the design of advanced fission and fusion reactors. Evolution on the microstructural scale is a consequence of the transport of point defects generated in energetic recoil events to various sinks within the microstructure, the segregation and aggregation of solutes as induced or accelerated by the super-saturations of such defects, and the accumulation and growth of sessile defect clusters. The exact response of a material depends on the conditions of exposure, such as temperature and radiation intensity, in addition to the properties of the material itself such as point defect energetics, chemistry and crystal structure, and the pre-existing microstructure.

Theoretical descriptions of radiation damage processes are complex, and must span the relevant time and length scales inherent in the problem from point defect generation and migration in femtosecond events on the atomic scale to property changes, which occur over the course of years or decades throughout nuclear reactor components on the engineering scale. The former is best handled through atomistic models, with density functional theory and molecular dynamics providing a wealth of information about energetic recoil cascades, point defect formation and migration energies, and other important aspects of the atomic level aspects of point defect behavior.

Changes in the physical and mechanical properties which might compromise the performance and reliability of structural materials result from the collective action of these defects, and understanding such processes requires a theoretical framework with a broader view than the atomic level is generally capable of providing. Evolution of the microstructure is governed by the accumulation, transport, and elimination of defects, as well as their mutual interactions, and interactions with the existing microstructure. Addressing the effects which occur over longer time scales (microns) and length scales (years) requires a model which can describe the density of defects which a particular irradiation condition will produce, account for the various interactions between them and the microstructure, and ultimately predict the consequent changes in the microstructure that can be expected.

The cluster dynamics (CD) modeling framework is one example of this type of model. Built upon mean field rate theory (MFRT), a fundamental modeling approach in radiation damage, CD has a wide variety of applications in modeling microstructural evolution. In this report, we first discuss the CD modeling framework before illustrating the results of the CD predictions for defect cluster evolution in irradiated ferritic-martensitic and austenitic alloys, respectively. The discussions of the CD results highlight the need for additional modeling improvements, which will be the focus of continuing work.

II. Cluster Dynamics Modeling Approach

The cluster dynamics simulation technique is well suited for modeling mesoscale microstructural evolution. Built on the fundamentals of the mean field rate theory analysis long used in an attempt to understand void swelling, these models track the density of point defects using partial differential equations of the form

$$\frac{dC_n}{dt} = D_n \nabla^2 C_n - D_n k_n^2 C_n - R_n\left(\vec{C}\right) + g_n$$

where for any species *n,* we can evolve its density *C* based on the diffusivity *D*, the sink strength for absorbing it k^2, the rate of production as primary damage *g*, and the rate at which it is created or destroyed by interaction with other defects *R(C)*. The reaction term can be expressed for a given species n,

$$R_n\left(\vec{C}\right) = \sum_{\substack{i+n\to m \\ n+i\to m}} k_{i,j}^{+} C_i C_n - \sum_{i+j\to n} k_{i,j}^{+} C_i C_j + \sum_{n-i\to j} k_{n,i,}^{-} C_n - \sum_{\substack{m-i\to n \\ m-j\to n}} k_{m,i}^{-} C_m$$

where the first term describes the loss of n through the combination of n with other clusters, the second term describes the formation of n through the combination of two reactant clusters, the third describes the loss of n by the dissociation of other clusters from it, and the forth term describes the formation of n by the dissociation of a parent cluster. The notation on the summations indicates the set of all possible (mass conservation) reactions (+) or dissociations (-). Accordingly, $k_{a,b}^{+}$ is the reaction rate coefficient between a and b, and $k_{a,b}^{-}$ is the dissociation rate constant for the emission of b from a. Generally, many clusters are capable of reaction and the relevant summations can produce significant coupling between the equations for various clusters.

In cluster dynamics, the evolution of certain classes of sinks is handled inherently by the growth of clusters to larger sizes with any change in sink strength reflected in the rate coefficients for the different clusters. For example, a cluster dynamics model would include distinct balance equations for the density of vacancy clusters of two, of three, of four, and so on up to thousands, millions or even billions of

constituents rather than a single equation governing the average size of the cavity. The cavity evolution is then described by a transfer of mass from smaller clusters to larger ones by absorbing vacancies, and from larger ones to smaller ones by absorbing self-interstitial atoms. Similarly, dislocation loop formation and growth manifests as the growth of the interstitial cluster distribution, and void swelling as the growth of the vacancy cluster distribution. Consequently, nucleation and growth of such sink classes are both described naturally in a cluster dynamics model, with no need for imposed nucleation models or other assumptions. Other sinks, such as network dislocations and grain boundaries remain external to the cluster distributions and are included in the sink strength term, k_n^2.

The other major advantage of cluster dynamics over its simpler rate theory predecessors is the ability to include cascade damage directly. Molecular dynamics simulations of energetic recoil events have indicated that for all but the lowest knock-on energies much of the damage is produced already in the form of extended clusters, in some cases with sizes extending to several dozen members. Depending on the material and its crystal structure, these clusters may be in the form of small cavities, stacking fault tetrahedra, dislocation loops of either a sessile or glissile character, and perhaps even more exotic lattice defects. Depending on the binding and migration energetics of these clusters, they may behave similarly to Frenkel pair analogues, may serve as immobile sink nuclei and/or recombination centers, or if in the form of a glissile dislocation loop may glide away from the cascade along one-dimensional trajectories. Early attempts to include such phenomenon in the traditional rate theory approach, collectively referred to as "production bias" models, indicated that considering this in-cascade clustering can have profound effects on the point defect partition and ultimately, predictions of microstructural evolution. In the cluster dynamics framework, in-cascade clustering is handled quite naturally, simply by supplying source terms *g* for as many clusters as necessary with the appropriate size distributions. Once again, cluster dynamics can handle all the subsequent defect behavior naturally, and for metals where the primary damage state is well characterized, no a priori assumptions about which clusters can dissociate to release free diffusing defects need to be made. Where the energetics of defect diffusion and dissociation processes are sufficiently well known, the reaction network indicated above resolves all such events.

III. Results and Discussion

Atomistic Modeling of Cavity Bias

In this work, the open source Large Array Molecular Massively Parallel Simulator (LAMMPS) [1] code was used. LAMMPS is a molecular dynamics (MD) code that can model large collections of particles using Newtonian mechanics and interactive force-fields between atoms through user provided interatomic potential functions. The interatomic potential selected for alpha Fe is from Mendelev et al. [2] since it correctly describes the ground state of the self-interstitial atom (SIA) as the <110> split-dumbbell. For the He-He and the Fe-He interactions, we have used the potentials from Janzen [3] and Juslin [4], respectively. The Fe-He potential correctly identifies the tetrahedral interstitial position as the ground state for interstitial helium in body-centered cubic Fe. Here we perform molecular statics (MS) calculations where an initial atomic configuration at 0 K is assessed for the lowest potential energy state. A minimization algorithm involving the conjugate gradient method is used to identify the lowest potential energy configuration. In LAMMPS, the atomic co-ordinates are iteratively adjusted until either the specified stopping tolerance or maximum number of iterations is reached.

First we examined the interaction distance for the spontaneous capture of an iron self-interstitial atom (SIA), vacancy or helium interstitial at a pure vacancy cluster (void) in body-centered cubic (BCC) iron as a function of the number of vacancies in the void. These results are presented in Figure 1, and include a variation of the center of mass position of the vacancy cluster on a lattice site versus either a tetrahedral or octahedral interstitial position. From Figure 1, it is clear that the interaction, or capture distance is largest for the iron self-interstitial atom (I, green symbols), and weakest fro the vacancy (V, reddish brown), with the helium interaction intermediate between the two intrinsic point defects. Given the weak dependence of the spontaneous capture distance on the size and configuration of the vacancy clusters, we selected a more limited set of sizes to investigate the temperature dependence of the interaction distance and the helium concentration within a cavity.

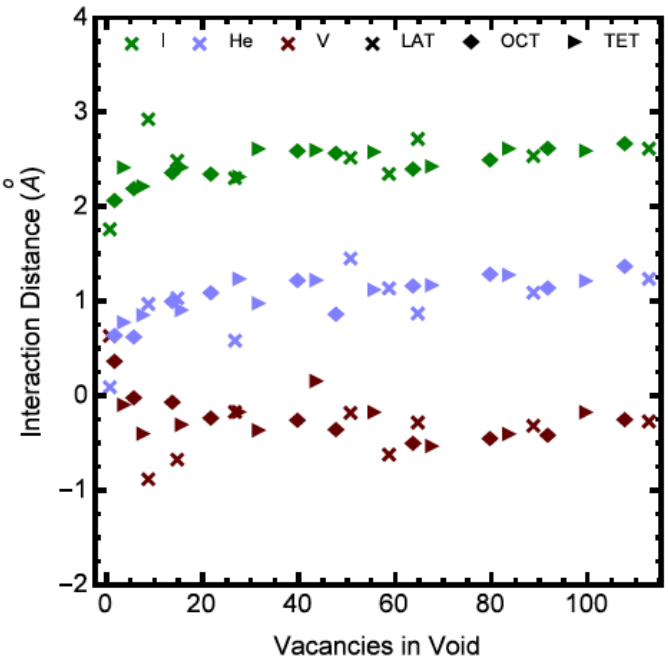

Figure 1. Interaction distance for the spontaneous capture of SIAs (I), vacancies (V) and helium (He) at vacancy clusters of various size with a center of mass on a lattice site (lat), or an octahedral (oct) or tetrahedral (tet) interstitial site.

Figure 2 shows the temperature dependence of the interstitial (SIA) versus vacancy (V) capture distance for a pure void containing 59 vacancies. The temperature dependence of the interaction, or capture, distance has been inferred from statics calculations by applying a thermal criterion wherein a point defect is considered to be captured if the interaction energy falls below –kT. The dashed lines in Fig. 2 show the spontaneous capture radii, which are assumed to be temperature independent. For attractive spherical interaction potentials, the effective capture radius is expected to scale as $T^{-1/3}$ for interaction energies that fall off as r^{-3}, as is the case for spherical cavities in an elastic medium. Thus, the calculated interaction radii in Fig. 2 have been fit to a homologous scaling law, $r_o = \alpha(T_m/T)^{1/3}$, where T_m is the melting temperature and α is the resulting fit parameter of 0.32 nm for SIA and 0.083 nm for a vacancy. These values of alpha correspond to approximately 4/3 and 1/3 of the nearest neighbor distance in BCC iron, respectively.

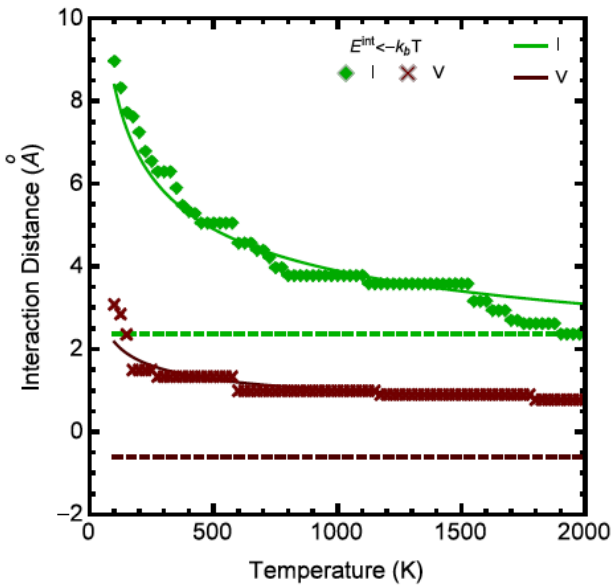

Figure 2. Interaction distance for the effective capture volume of a 59-member void for SIA (I) and vacancy (V) point defects as a function of temperature. The dashed lines show the spontaneous capture volumes.

As shown in Figure 2, the effective capture radius for SIAs at an 59-member void approach the spontaneous value at temperatures near the melting point, while the vacancies experience a slightly extended capture volume throughout the examined range. As temperature decreases however, the interstitial interaction distance increases much more rapidly than that of the vacancy. The optimal temperature range for void swelling in BCC iron based alloys is generally observed to occur around 700 K, in both neutron and heavy ion irradiation experiments [5-7], and in this range, the interaction radius for SIA absorption at a void is nearly double the spontaneous capture radius and is nearly 3 times larger than the effective interaction/capture radius of the vacancy.

To investigate the effect of helium on the defect capture radii for cavities, molecular statics calculations for 59 and 113 member vacancy clusters were performed with various amounts of helium. The interaction distances for spontaneous capture at these bubbles are shown in Figure 3 as a function of gas pressure using the dimensionless measure $pa_0/2\gamma$, with the pressures spanning site filling ratios up to slightly more than 2 He per vacancy [8]. For both cavity sizes the spontaneous capture radius for SIAs did not change dramatically in response to the introduction of gases. Vacancies, on the other hand, were absorbed into the bubble at significantly larger distances as the gas pressure increased with an apparently linear trend. The increase did not begin until the bubbles were over-pressurized, and at lower pressures, the interaction distance has an approximately constant value. No discernible difference between the two bubble sizes was evident in the linear region, although the minimum capture radius for under-pressurized bubbles varied slightly.

To formulate an analytical expression for the bias of bubbles,

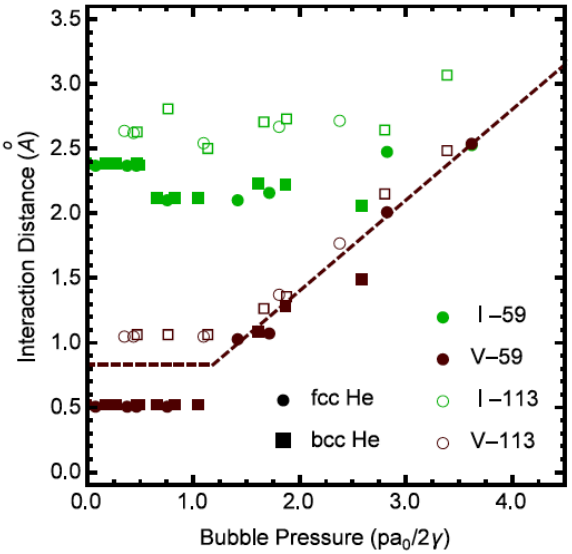

Figure 3. Interaction distance for the spontaneous capture of SIA (I) and vacancy (V) point defects at gas bubbles using a Wigner-Seitz criterion as a function of the gas pressure. Data for bubbles filling 69 or 113 vacancies are shown. A fit to the vacancy data following a linear increase in capture distance is shown with increasing helium gas pressure.

we fit the region of linear increase and applied this expression to the alpha interaction distance discussed previously, with an additional temperature dependent helium gas pressure within the bubble. The results of the vacancy interaction distance and corresponding analytical fitting expression are shown in Figure 4 for several different helium gas pressures (shown in units of $pa_o/2\gamma$, where a_o is the lattice constant and γ is the surface tension of the material). In comparing Figures 3 and 4, it is apparent that the interaction distance for vacancies does not approach the value for SIAs until the highest gas pressures are reached, indicating that a neutral bias is not obtained until bubbles are near the pressure required for trap mutation or dislocation loop punching. However, it is possible that screening SIAs through repulsive interactions may allow for a neutral bias somewhat closer to the equilibrium pressure, but definitely not for under-pressurized bubbles. Future atomistic modeling will begin to address additional questions related to the role of impurities and other microstructural features on the inherent bias of the bubbles.

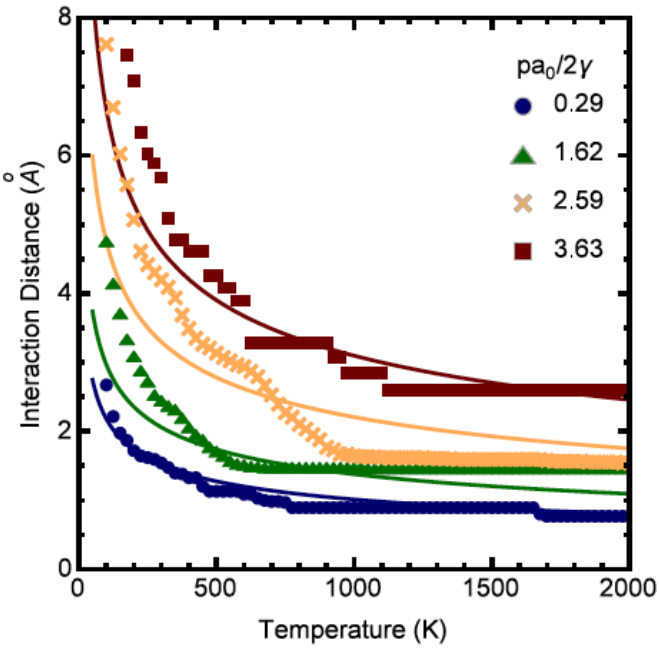

Figure 4. Interaction distance for the effective capture of vacancies to a bubble as a function of gas pressure and temperature, as compared to an analytical model for the temperature and pressure dependence given by the solid lines.

<u>Cluster Dynamics Model Predictions of the Effect of Cavity Bias</u>

Figure 5 shows an example of implementing this concept of cavity bias to evaluate the influence of He production, coupled with heavy ion irradiation, on the onset of swelling in Fe-Cr based ferritic-martensitic alloys. In this work, we have informed our cluster dynamics model with atomistic data on the thermodynamics and kinetics of helium – defect clusters, as well as taken into account the production of defect clusters directly in high-energy displacement cascades, and utilized a mostly forgotten concept that small vacancy clusters, including those containing

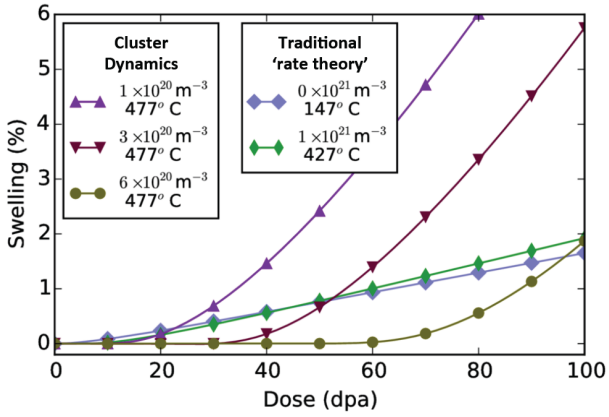

Figure 5. Cluster dynamics predictions of swelling versus radiation dose in an Fe-9%Cr ferritic-martensitic alloy subject to dual ion irradiation conditions (up & down triangles, circles), as compared to traditional rate theory (blue & green diamonds). Irradiation temperature and density of heterogeneous nucleation sites are provided in the legend.

an internal gas pressure, are actually biased sinks for absorption of self-interstitial atoms relative to vacancies [9]. Our model also incorporates a specified number of heterogeneous nucleation sites for cavities. The family of three curves (up and down triangles, circles, respectively) are predictions of our model using different densities of heterogeneous nucleation sites, and naturally predict the onset of a critical incubation dose prior to essentially constant swelling rate at an irradiation temperature of 477°C. Our modeling predictions should be compared to the more traditional rate theory solutions (blue and green diamonds) at low versus higher temperature, and with, or without, heterogeneous nucleation sites, respectively, which do not agree well with experimental observations.

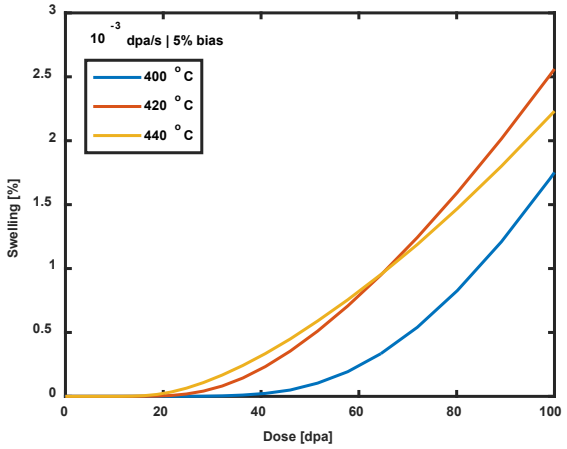

Figure 6. Cluster dynamics predictions of swelling versus radiation dose in BCC iron for ion irradiation at temperatures of 400, 420 and 440 °C (blue, red and yellow lines, respectively). These calculations used a dislocation bias of 5%.

As well, Figure 6 shows the results of applying this cluster dynamics model including cavity bias to a case of ion irradiation with a dose rate of 10^{-3} dpa/sec and using a 5% dislocation bias, as a function of irradiation temperature from 400 to 440 °C. The incorporation of the cavity bias for SIA absorption naturally introduces an incubation period for the onset of void swelling, which is observed to decrease with increasing temperature. Although not shown here, the same cluster dynamics model for ion irradiation and 5% dislocation does not predict an incubation dose without incorporating the effect of cavity bias. In those cluster dynamics simulation results, the level of swelling is increased by at least an order of magnitude relative to the values predicted in Fig. 6. While these initial results are promising, future efforts will continue to expand evaluation of this effect of cavity and bubble bias on the implications for radiation-induced swelling of structural materials in high dose fast reactor neutron environments, with an emphasis on extending the atomistic modeling to evaluate the impact of self-interstitial cluster absorption, the role of impurity atoms in mitigating the bias effect by screening the displacement (stress) fields and benchmarking the cluster dynamics modeling predictions to a wider set of experimental data.

IV. Conclusions

This report describes the implementation of a new model for biased absorption of self-interstitial atoms by small cavities, including those that contain helium gas pressure, into cluster dynamics models. Following a description of the atomistic modeling results that document the bias, an initial set of cluster dynamics results has been presented that indicates the potential for this new modeling approach to successfully reproduce the incubation period for the onset of swelling that is experimentally observed in irradiated steels. Future work will emphasize extending the atomistic modeling to evaluate the impact of self-interstitial cluster absorption, the role of impurity atoms in mitigating the bias effect by screening the displacement (stress) fields and benchmarking the cluster dynamics modeling predictions to a wider set of experimental data.

V. References

[1] S. Plimpton, *J. Comput. Phys.* **117** (1993) 1-19.
[2] M.I. Mendelev, S. Han, D.J. Srolovitz, G.J. Ackland, D.Y. Sun, and M. Asta, *Philos. Mag.* **83** (2003) 3977-3994.
[3] A.R. Janzen and R.A. Aziz, *J. Chem. Phys.* **107** (1997) 914.
[4] N. Juslin and K. Nordlund, *J. Nucl. Mater.* **382** (2008) 143-146.
[5] E.A. Little, R. Bullough and M.H. Wood, *Proc. R. Soc. A. Math, Phys. Eng. Sci.* **372** (1980) 565-579.
[6] D.S. Gelles, *J. Nucl. Mater.* **225** (1995) 163-174.
[7] E. Getto, Z. Jiao, A. Moterrosa, K. Sun, and G.S. Was, *J. Nucl. Mater.* **465** (2015) 116-126.
[8] A.A. Kohnert, M.A. Cusentino and B.D. Wirth, *J. Nucl. Mater.* **499** (2018) 480-489.